

Channel Characterisation of Cooperative Relaying Power Line Communication Systems

Matjaz Rozman, Augustine Ikpehai, Bamidele Adebisi, Khaled M. Rabie
School of Engineering, Division of Electrical Engineering

Manchester Metropolitan University, M1 5GD UK

Emails: {matjaz.rozman, augustine.ikpehai}@stu.mmu.ac.uk; {b.adebisi, k.rabie}@mmu.ac.uk

Abstract—Power line communication (PLC) technology offers a promising platform for numerous communication applications. The power lines however can significantly attenuate communication signals operating in high frequency band. For this reason, multi-hop PLC systems become desirable. In this paper, we investigate the effect of multi-hop relaying on the power line channel transfer function. Measured results are compared with results obtained from simulations in Matlab. Results show that the presence of relays between a transmitting and a receiving PLC nodes can intensify the attenuation and frequency selectivity. Measurements show that maximum attenuation increases with number of relays.

Keywords—PLC, relay-assisted, multi-hopping, channel characterisation

I. INTRODUCTION

Power line communication (PLC) technology is attractive for data transmission in indoor and outdoor data communication networks [1]. Research on PLC started in late 1990's; and recently, due to the high power demand, a major effort has been deployed towards achieving *smart grid*. Communication link reliability is a major factor in designing the next-generation energy infrastructure. In-home PLC can also help to improve home energy management by enabling exchange of messages. Power line channels are highly available, and can provide broadband data transmission. Together with smart devices, PLC can facilitate realisation of smart buildings.

However, due to the high number of electrical devices and the distance between them, the use of relaying becomes inevitable in cases where direct communication is either unachievable or unreliable. Similar to wireless communications, relaying in PLC can be employed to improve throughput and increase the coverage area. It is worth nothing that relaying is not as effective over power line channels compared to wireless systems due the lack of diversity improvement [2]. In addition, the position of the relay is a key factor for maximum energy efficiency [3].

As demonstrated in [4], relay assisted PLC consists of two keyhole channels and thus can't be compared to wireless. Despite its relative lower efficiency, relay assisted PLC can enhance system performance in many scenarios. According to [5], an intermediate node between transmitter and receive helps to improve performance via opportunistic relaying.

While cooperative assisted PLC can improve channel capacity on the one hand, it has some limitations on the other. In [6], it was numerically demonstrated and concluded that in order to improve the coverage in in-home PLC, the relay should not be placed far from the source and destination and

relaying is recommended to improve performance only when the channel conditions of direct transmission paths are not favorable.

The quality of service (QoS) in PLC rely on the channel characteristic. Considerable amount of research has been conducted on channel characterisation of power lines, such as in [7, 8, 9, 10], where researchers analysed the effect of notches, length, and distance between the source and destination on transfer function of the channel. Furthermore, the authors in [11] and [12], have investigated the low voltage single phase channel transfer function and mathematically described it.

In contrast, this paper focuses on multiple relays PLC system. The contribution of this paper resides in providing a mathematical model and building a test circuit. A comparison between the numerical and measured results is then made. It has been shown that the presence of relays can have a negative effect on channel transfer function.

The remaining of this paper is organised as follows. Section II describes the in-home power line network and derives mathematical transmission matrices and transfer functions associated with each transmission path. Section III discusses the experimental setup used in this work while in section IV results are discussed. Finally, the main conclusions of work are highlighted in section V.

II. TOPOLOGY OF BUILDING POWER LINE SYSTEM

In-home wiring regulations and technical standards in the UK are described in standardised BS 7671-2008. Typical topology for UK in-home power line system in residential buildings and wiring practices can be seen in Fig 1. Outlet sockets in one room are fed by the same power supply and are placed parallel to each other, while lights in each room are fed by own power supply directly from the main consumer unit.

As illustrated in Fig. 1, control messages can typically be sent from a management station in the home to turn on/off the light or deactivate supply to socket(s) in a bid to regulate energy consumption. In certain cases, such direct communication is difficult or impossible to achieve. Communication between two devices can be improved by employing an additional node to mediate between the management station (source) and the light or socket (destination); this is the concept of multi-hopping or relaying. In such cases, the relay can be positioned on different sockets and in case of multiple-floor houses, even in different floors. The resulting network comprises of a source (S), one or more relays (R) and a destination (D), is shown in Fig. 2.

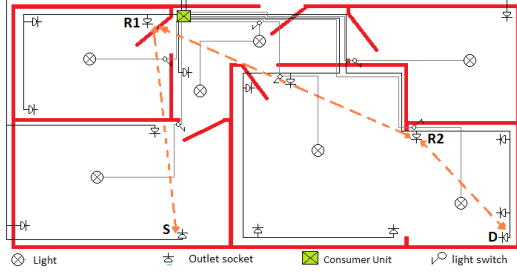


Fig. 1. Building power line network topology

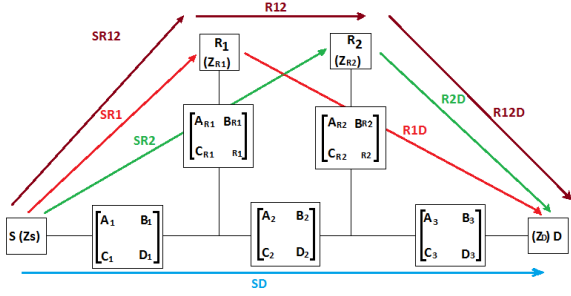


Fig. 2. Cooperative relay network model

A. Direct Path from Source to Destination

Consider the direct path from the source to the destination (SD), see Fig. 2. SD path resides on the main channel line and exhibits channel characteristics different from other paths through the branches. The impedance of each branch can be expressed as

$$Z_{eqbr_i} = \frac{A_{Ri}Z'_{LRi} + B_{Ri}}{C_{Ri}Z'_{LRi} + D_{Ri}} \quad (1)$$

where the A_{Ri} , B_{Ri} , C_{Ri} and D_{Ri} represent the transmission matrix parameters of the relay branch while i is the index of the branch. Z'_{LRi} , which represents the equivalent impedance at the relay consists of Z_{Ri} and Z_{LRi} connected in parallel, therefore can be calculated as

$$Z'_{LRi} = \frac{Z_{Ri}Z_{LRi}}{Z_{Ri} + Z_{LRi}} \quad (2)$$

The transmission matrix for the direct path can be expressed as

$$\begin{aligned} T_{SD}^D &= \begin{bmatrix} A_{SD}^D & B_{SD}^D \\ C_{SD}^D & D_{SD}^D \end{bmatrix} \\ &= \begin{bmatrix} 1 & 0 \\ Z_S & 1 \end{bmatrix} \begin{bmatrix} A_1 & B_1 \\ C_1 & D_1 \end{bmatrix} \begin{bmatrix} 1 & 0 \\ \frac{1}{Z_{eqbr1}} & 1 \end{bmatrix} \\ &\quad \begin{bmatrix} A_2 & B_2 \\ C_2 & D_2 \end{bmatrix} \begin{bmatrix} 1 & 0 \\ \frac{1}{Z_{eqbr2}} & 1 \end{bmatrix} \begin{bmatrix} A_3 & B_3 \\ C_3 & D_3 \end{bmatrix} \end{aligned} \quad (3)$$

and the path gain for SD is given by

$$H_{SD}^D = \frac{Z_L}{A_{SD}^D Z_L + B_{SD}^D + C_{SD}^D Z_L Z_S + D_{SD}^D Z_S} \quad (4)$$

B. Path Through First Relay

A path through a relay can be described as a connection between two paths to a midpoint between source and destination. When the signal travels from the source to R1, R1 is considered as destination while R2 and D jointly behave as a branch. Therefore, the branch impedance can be considered as the sum of impedance of R2 and D. Hence, the impedance of R2 can be derived from (1) while the impedance of D is calculated as

$$Z_{Deq} = \frac{A_3 Z'_L + B_3}{C_3 Z'_L + D_3} \quad (5)$$

R2 and D are connected in parallel, hence, their resultant impedance can be expressed as:

$$Z_{FDR2} = \frac{Z_{eqbr2} Z_{Deq}}{Z_{eqbr2} + Z_{Deq}} \quad (6)$$

and the impedance of the whole branch Z_{FDR2eq} (formed between R2 and D) can be calculated

$$Z_{FDR2eq} = \frac{A_2 Z_{FDR2} + B_2}{C_2 Z_{FDR2} + D_2} \quad (7)$$

combined with the second relay impedance expressed in (1), the path matrix can be written as

$$\begin{aligned} T_{SR1}^1 &= \begin{bmatrix} A_{SR1}^1 & B_{SR1}^1 \\ C_{SR1}^1 & D_{SR1}^1 \end{bmatrix} = \begin{bmatrix} 1 & 0 \\ Z_S & 1 \end{bmatrix} \\ &\quad \begin{bmatrix} A_1 & B_1 \\ C_1 & D_1 \end{bmatrix} \begin{bmatrix} 1 & 0 \\ \frac{1}{Z_{FDR2eq}} & 1 \end{bmatrix} \begin{bmatrix} A_{R1} & B_{R1} \\ C_{R1} & D_{R1} \end{bmatrix} \end{aligned} \quad (8)$$

Path gain between S and R1 is

$$H_{SR1}^1 = \frac{Z_{R1}}{A_{SR1}^1 Z_{R1} + B_{SR1}^1 + C_{SR1}^1 Z_{R1} Z_S + D_{SR1}^1 Z_S} \quad (9)$$

Additionally, we consider the path from R1 to D in which R1 behaves as the source and D remains the destination where S and R2 become branches. In this case, the impedance of S can be calculated as

$$Z_{Seq} = \frac{A_1 Z_S + B_1}{C_1 Z_S + D_1} \quad (10)$$

and the ABCD matrix can be written as

$$\begin{aligned} T_{SR1}^2 &= \begin{bmatrix} A_{SR1}^2 & B_{SR1}^2 \\ C_{SR1}^2 & D_{SR1}^2 \end{bmatrix} \\ &= \begin{bmatrix} 1 & 0 \\ Z_{R1} & 1 \end{bmatrix} \begin{bmatrix} A_{R1} & B_{R1} \\ C_{R1} & D_{R1} \end{bmatrix} \begin{bmatrix} 1 & 0 \\ \frac{1}{Z_{Seq}} & 1 \end{bmatrix} \\ &\quad \begin{bmatrix} A_2 & B_2 \\ C_2 & D_2 \end{bmatrix} \begin{bmatrix} 1 & 0 \\ \frac{1}{Z_{eqbr2}} & 1 \end{bmatrix} \begin{bmatrix} A_3 & B_3 \\ C_3 & D_3 \end{bmatrix} \end{aligned} \quad (11)$$

and the path gain is given as

$$H_{SR1}^2 = \frac{Z_L}{A_{SR1}^2 Z_L + B_{SR1}^2 + C_{SR1}^2 Z_L Z_{R1} + D_{SR1}^2 Z_{R1}} \quad (12)$$

Finally, the composite path gain of the entire S-R1-D, consisting of S-R1 and R1-D paths, can be expressed as the sums of the two path gains expressed as

$$H_{SD}^{R1} = (H_{SR1}^1 A) + H_{SR1}^2 \quad (13)$$

where A represents amplifying ratio if amplify and forward relay is in use.

C. Path Through Second Relay

Similar to (2), the path through second relay can be described as the signal propagation from the S through R2 to D. On receiving the signal, R2 forwards it to D. Therefore, in the first part R2 acts as a signal destination while R1 and D combined act as a branch. Mathematically, the branch impedance of R1 can be calculated using (1). Similarly, the equivalent impedance of D is calculated using (5). The transmission $ABCD$ matrix can be expressed as

$$\begin{aligned} T_{SR2}^1 &= \begin{bmatrix} A_{SR2}^1 & B_{SR2}^1 \\ C_{SR2}^1 & D_{SR2}^1 \end{bmatrix} \\ &= \begin{bmatrix} 1 & 0 \\ Z_S & 1 \end{bmatrix} \begin{bmatrix} A_1 & B_1 \\ C_1 & D_1 \end{bmatrix} \begin{bmatrix} 1 & 0 \\ \frac{1}{Z_{eqbr1}} & 1 \end{bmatrix} \\ &\quad \begin{bmatrix} A_2 & B_2 \\ C_2 & D_2 \end{bmatrix} \begin{bmatrix} 1 & 0 \\ \frac{1}{Z_{Deq}} & 1 \end{bmatrix} \begin{bmatrix} A_{R2} & B_{R2} \\ C_{R2} & D_{R2} \end{bmatrix} \quad (14) \end{aligned}$$

and the path gain

$$H_{SR2}^1 = \frac{Z_{R2}}{A_{SR2}^1 Z_{R2} + B_{SR2}^1 + C_{SR2}^1 Z_{R2} Z_S + D_{SR2}^1 Z_S} \quad (15)$$

Considering the path from R2 to D, S and R1 jointly behave as a branch. The equivalent impedance at S can be derived from (10) and S is now parallel to R1 and impedance of R1 can be calculated using (1). Furthermore, the impedance of the branch can be calculated as parallel impedance connection of R1 and S as

$$Z'_{SR1} = \frac{Z_{eqbr1} Z_{Seq}}{Z_{eqbr1} + Z_{Seq}} \quad (16)$$

and the impedance of the whole branch (formed by R1 and S) is calculated

$$Z_{SR1} = \frac{A_2 Z'_{SR1} + B_2}{C_2 Z'_{SR1} + D_2} \quad (17)$$

The $ABCD$ matrix is given by:

$$\begin{aligned} T_{SR2}^2 &= \begin{bmatrix} A_{SR2}^2 & B_{SR2}^2 \\ C_{SR2}^2 & D_{SR2}^2 \end{bmatrix} = \begin{bmatrix} 1 & 0 \\ Z_{R2} & 1 \end{bmatrix} \\ &\quad \begin{bmatrix} A_{R2} & B_{R2} \\ C_{R2} & D_{R2} \end{bmatrix} \begin{bmatrix} 1 & 0 \\ \frac{1}{Z_{SR1}} & 1 \end{bmatrix} \begin{bmatrix} A_3 & B_3 \\ C_3 & D_3 \end{bmatrix} \quad (18) \end{aligned}$$

Now, the path gain on R2-D can be described as:

$$H_{SR2}^2 = \frac{Z_L}{A_{SR2}^2 Z_L + B_{SR2}^2 + C_{SR2}^2 Z_L Z_{R2} + D_{SR2}^2 Z_{R2}} \quad (19)$$

Again the whole path of the connection through R2 can be calculated as a sum of the two parts:

$$H_{SD}^{R2} = (H_{SR2}^1 A) + H_{SR2}^2 \quad (20)$$

D. Path Through First and Second Relay

In this section, the connection through both relays is considered. Here, the signal propagation is considered in three stages. In the first stage, S sends the signal to R1. R2 and D are considered as branches and their equivalent impedance is calculated using (7).

In the second stage, the communication signal originates from R1, which is now considered as the source of the signal, to R2, now considered as the destination. S and D now form a branch on the network. The equivalent impedance of S is given in (10), while the impedance of D can be calculated using (5). Therefore, the $ABCD$ matrix for the considered path can be written as

$$\begin{aligned} T_{SR12}^2 &= \begin{bmatrix} A_{SR12}^2 & B_{SR12}^2 \\ C_{SR12}^2 & D_{SR12}^2 \end{bmatrix} \\ &= \begin{bmatrix} 1 & 0 \\ Z_{R1} & 1 \end{bmatrix} \begin{bmatrix} A_{R1} & B_{R1} \\ C_{R1} & D_{R1} \end{bmatrix} \begin{bmatrix} 1 & 0 \\ \frac{1}{Z_{Seq}} & 1 \end{bmatrix} \\ &\quad \begin{bmatrix} A_2 & B_2 \\ C_2 & D_2 \end{bmatrix} \begin{bmatrix} 1 & 0 \\ \frac{1}{Z_{Deq}} & 1 \end{bmatrix} \begin{bmatrix} A_{R2} & B_{R2} \\ C_{R2} & D_{R2} \end{bmatrix} \quad (21) \end{aligned}$$

The path gain can be mathematically calculated as

$$H_{SR12}^2 = \frac{Z_{R2}}{A_{SR12}^2 Z_{R2} + B_{SR12}^2 + C_{SR12}^2 Z_{R2} Z_{R1} + D_{SR12}^2 Z_{R1}} \quad (22)$$

The last part of the communication path is from R2 to D. In this case, R2 behaves as a source of information and R1 and S are considered as a branch whose equivalent impedances are given by (16) and (17), respectively.

As with previous subsections, the path gain of the whole path can be calculated as a sum of all three paths previously which can be expressed as

$$H_{SD}^{R12} = (H_{SR1}^1 A) + (H_{SR12}^2 A) + (H_{SR2}^2) \quad (23)$$

III. EXPERIMENTAL SETUP

This section describes the network setup employed in this work. Five network topologies are created in the laboratory as shown in Fig. 3. These topologies are based on possible use scenarios of multiple relays in an in-building power line network. In the first scenario, both relays located on the branches and both branches located close to the source as illustrated in Fig. 3a. In the second scenario, R1 is connected to the short branch while R2 is connected directly to the main line, see Fig.3b. In the third case, relay R1 is connected directly on the main line while R2 is connected to the long branch as shown in Fig. 3c. Next, both relays are connected directly on the main line as demonstrated in Fig. 3d. Finally, a case is considered in which R2 is closer to D than S as shown in Fig.3e.

Each channel occupies the frequency band from 1.7MHz to 30MHz. Our aim here is to measure and compare line attenuation among the different topologies as well as the transmission paths. Although the use of relay is well established in wireless communication, the effect of multiple relays on the transmission line transfer characteristics is of interest in this work. It will be shown in the next section that indeed, there

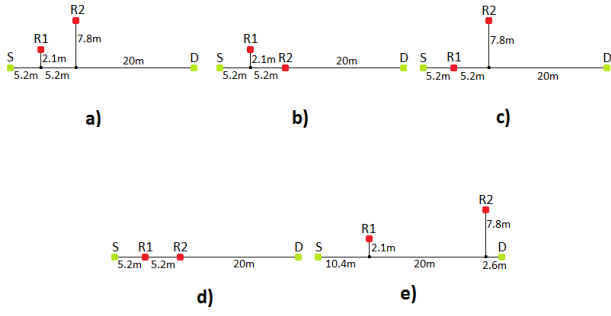


Fig. 3. Measured power line topologies

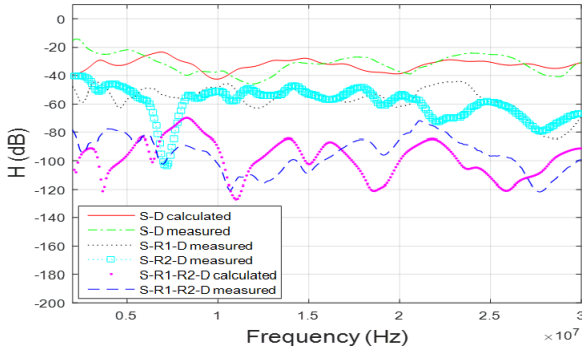


Fig. 4. Comparison between measured and simulated results while R1 and R2 are connected to a branch (topology 3a)

is a correlation and some trade-off between the use of relay and path attenuation.

IV. RESULTS

In this section, we present and compare simulation results of various system configurations under consideration.

A. Case 3a: R1 and R2 connected to branches

In this scenario, relays R1 and R2 are positioned at 5.2m and 10.4m respectively from S. Lengths of the branches are 2.1m (short branch) and 7.8m (long branch) for R1 and R2 respectively as shown in Fig. 3a. Fig. 4 presents some measured results for S-D, S-R1-D, S-R2-D and S-R1-R2-D and calculated results for S-D and S-R1-R2-D paths. It can be seen from the figure that when R2 is connected, the channel transfer function degrades compared to the S-R1-D path. It can be also that with R1 and R2 connected on branches close the S, the depth of the notches increases from about -47.5dB in case of (S-D) to -121dB implying additional loss of 73.5dB for the transmission line with both relays. In the case of S-R1-D and S-R2-D, maximum attenuation are -84dB and -103dB, respectively.

B. Case 3b: R1 on the short branch and R2 the main line

This scenario employs the topology illustrated in Fig. 3b. Fig. 5 presents measured and calculated results for direct path S-D, measured results through R1 and R2, measured and calculated results for S-R1-R2-D paths. As can be seen from Fig. 5, the path through relay R2, which connects to the main

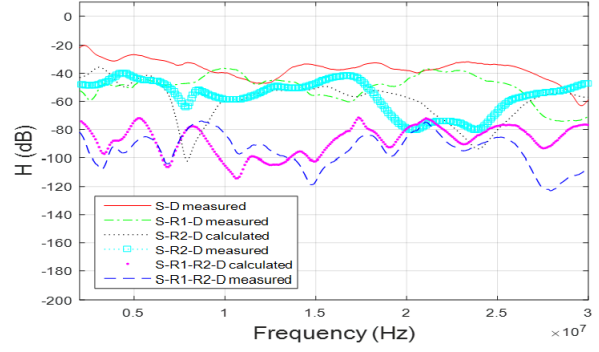


Fig. 5. Comparison between measured and simulated results when R1 is located on the branch while R2 is connected to the main line (topology 3b)

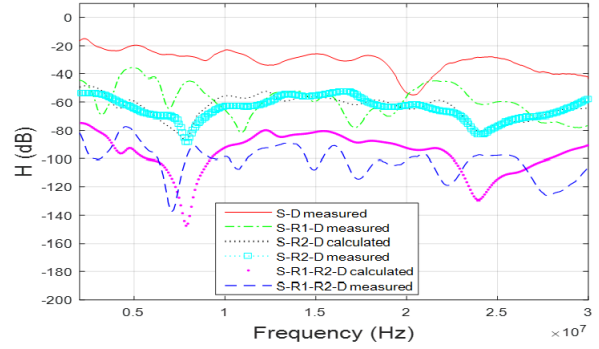


Fig. 6. Comparison between measured and simulated results when R1 connected on the main line and R3 on a long branch (topology c)

line experiences more attenuation (-80 dB) compared to the path through R1 (-76 dB). Further, we can see that the path through both relays have a maximum attenuation of -122dB.

C. Case 3c: R1 on main line, R2 on long branch

In this experiment, the setup in Fig. 3c is employed but R1 is now connected directly to the main line. In Fig. 6, measured results of S-D, S-R1-D, S-R2-D, S-R1-R2-D paths and calculated results of S-R2-D and S-R1-R2-D are presented. From the Fig. 5, it is evident that the S-R1-D path experiences maximum attenuation of -80.5dB compared with and R2 with -85dB. It can also be seen that the path through R1 and R2 exhibits the highest loss with peak attenuation of -138dB, making it worse than the cases 4a and 4b.

D. Case 3d: R1 and R2 on the main line

In this case, the topology in Fig. 3d in which both relays connect directly to the main transmission line applies. Fig. 7 illustrates the measured results of S-D, S-R1-D, S-R2-D, S-R1-R2-D paths and calculated results of S-R1-D and S-R1-R2-D paths. While S-R1-D and S-R2-D show a maximum attenuation of -83dB and -67dB, respectively, the performance is worse on the transmission line with R1 and R2 as the line attenuation increases to -133dB.

E. Case 3e: R2 is connected closer to the destination

Unlike cases 4a-d, in this experiment, we change the position of R2 by moving it closer to D than S and investigate the

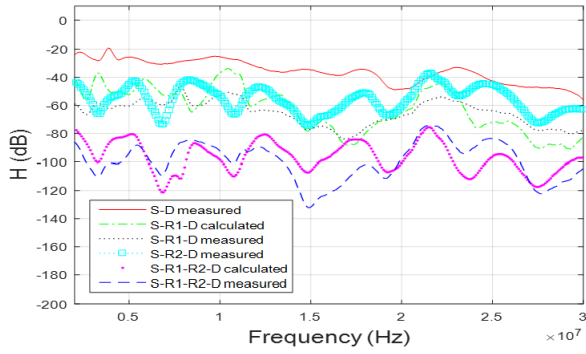


Fig. 7. Comparison between measured and simulated results when R1 and R2 connected on the main line (topology d)

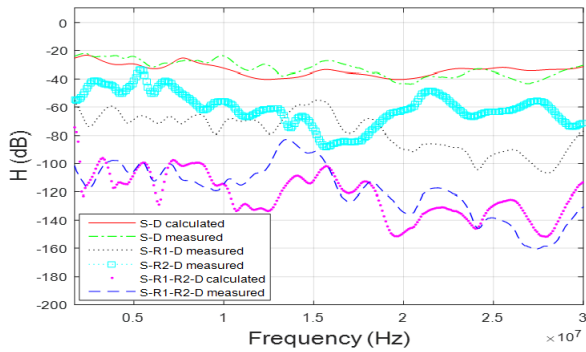


Fig. 8. Comparison between measured and simulated results when R2 is connected closer to the destination (topology e)

effect of a such relocation. Fig. 8 depict the measured results of S-D, S-R1-D, S-R2-D, S-R1-R2-D paths and calculated results of S-D and S-R1-R2-D. It can be seen from Fig.8 that when the second branch is connected closer to its destination with R2 on it, maximum line attenuation of S-R1-D, S-R2-D, S-R1-R2-D are -108dB, -89dB and -160dB, respectively. The main observation here is that S-R1-D and S-R1-R2-D experience the highest attenuation in case 4e than in previous four cases.

V. CONCLUSIONS

It can be concluded that the use of relays can potentially improve coverage and throughput of PLC systems. However, multiple relays between transmitter and receiver involves some performance trade-off. It has been shown in this paper that, compared with direct paths and paths with single relay, the use of two relays results in higher attenuation. It has also been presented (case 4e) that position of the relay relative to the transmitter or receiver can affect transfer characteristics of the transmission line. The significance of these results is that although multiple relays can generally improve communication performance, the direct path remains the preferred option. Multiple relays should be employed only when direct path is either unavailable or significantly inefficient.

ACKNOWLEDGMENT

These investigations were carried out within research activities funded by the Innovate UK under the “Smart In-Building

Micro Grid for Energy Management” project (Innovate UK Project 101836).

REFERENCES

- [1] A. M. Tonello and F. Versolatto, “Bottom-up statistical PLC channel modeling ;part i: Random topology model and efficient transfer function computation,” *IEEE Trans. on Power Del.*, vol. 26, no. 2, pp. 891–898, Apr. 2011.
- [2] M. Noori and L. Lampe, “Multi-way relaying for cooperative indoor power line communications,” *IET Commun.*, vol. 10, no. 1, pp. 72–80, Feb. 2016.
- [3] W. Bakkali, P. Pagani, and T. Chonavel, “Energy efficiency performance of relay-assisted power-line communication networks,” in *IEEE Consumer Commun. and Networking Conf. (CCNC)*, Jan. 2015, pp. 525–530.
- [4] L. Lampe and A. J. H. Vinck, “Cooperative multihop power line communications,” in *IEEE Int. Symp. Power Line Commun. and Its Appl. (ISPLC)*, Mar. 2012, pp. 1–6.
- [5] A. M. Tonello, F. Versolatto, and S. D’Alessandro, “Opportunistic relaying in in-home PLC networks,” in *IEEE Global Telecommun. Conf. (GLOBECOM)*, Dec. 2010, pp. 1–5.
- [6] M. S. P. Facina, H. A. Latchman, H. V. Poor, and M. V. Ribeiro, “Cooperative in-home power line communication: Analyses based on a measurement campaign,” *IEEE Trans. on Commun.*, vol. 64, no. 2, pp. 778–789, Feb. 2016.
- [7] K. Kale and S. K. Patra, “Characterization of broadband power line channel,” in *Global Conf. Commun. Technol.*, Apr. 2015, pp. 673–677.
- [8] L. Wang, G. Avolio, G. Deconinck, E. V. Lil, and L. L. Lai, “Estimation of multi-conductor powerline cable parameters for the modelling of transfer characteristics,” *IET Sci., Meas. Technol.*, vol. 8, no. 1, pp. 39–45, Jan. 2014.
- [9] Z. Jie, Y. Xiao, and Q. Kaiyu, “Research on characteristics of low voltage power line communication channel,” in *IEEE Power Engin. and Automat. Conf. (PEAM)*, Sept. 2012, pp. 1–5.
- [10] B. Adebisi, S. Ali, and B. Honary, “Multi-emitting/multi-receiving points mmfsk for power-line communications,” in *Power Line Commun. and Its Applicat., 2009. ISPLC 2009. IEEE Int. Symp. on*, Mar. 2009, pp. 239–243.
- [11] H. Meng, S. Chen, Y. L. Guan, C. L. Law, P. L. So, E. Gunawan, and T. T. Lie, “Modeling of transfer characteristics for the broadband power line communication channel,” *IEEE Trans. on Power Delivery*, vol. 19, no. 3, pp. 1057–1064, Jul. 2004.
- [12] S. Wei, D. Liu, X. Xu, X. Yang, and Y. Chang, “Research of channel characteristics of the low voltage power line under the coal mine,” in *Int. Congress Image and Signal Proc. (CISP)*, vol. 03, Dec. 2013, pp. 1372–1375.